A Compact Dual-Band Antenna Design Using a Non-Uniform Inverted U-Shaped DGS and an Efficient Quasi-Oppositional Grey Wolf Optimizer

Wellington Ochieng
Department of Electrical and Information Engineering, Faculty of Engineering, University of Nairobi, Nairobi, Kenya
akelowellington@gmail.com (corresponding author)

Davies Segera
Department of Electrical and Information Engineering, Faculty of Engineering, University of Nairobi, Nairobi, Kenya
davies.segera@uonbi.ac.ke

Abraham Nyete
Department of Electrical and Information Engineering, Faculty of Engineering, University of Nairobi, Nairobi, Kenya
anyete@uonbi.ac.ke

Received: 15 July 2025 | Revised: 9 August 2025 | Accepted: 22 August 2025

 DOI: https://doi.org/10.48084/etasr.13409

ABSTRACT

In this study, a non-uniform inverted U-shaped Defected Ground Structure (DGS) was used to optimize a dual-band, compact microstrip antenna for operation at 2.6 GHz and 3.5 GHz frequency bands, which are widely used for sub-6 GHz 5G applications. Because the design of DGS-based antennas usually involves iterative optimization and extensive full-wave simulations, an Efficient Quasi-Oppositional Grey Wolf Optimizer (EQOGWO) is proposed to reduce the computational cost. The EQOGWO achieves high-quality solutions with fewer evaluations than the Grey Wolf Optimizer (GWO). The antenna comprises symmetrical open slots on a rectangular patch and an L-shaped parasitic element. The designed antenna attained a simulated S_{11} value of −20.4 dB at 2.6 GHz and −25.69 dB at 3.5 GHz, meeting the target of a maximum of −10 dB within the operating frequency ranges.

Keywords-Defected Ground Structure (DGS); Grey Wolf Optimizer (GWO); Efficient Quasi-Oppositional Grey Wolf Optimizer (EQOGWO)

I. INTRODUCTION

Compact antennas have become increasingly important in today's highly connected world. However, achieving the required performance often necessitates a Multiple-Input Multiple-Output (MIMO) configuration, which further increases the challenge of minimizing the antenna footprint. When antennas cannot be sufficiently spaced due to compactness constraints, various decoupling techniques can be employed, such as adding isolation structures including a neutralization line, a parasitic element, or a Defected Ground Structure (DGS). In addition to reducing coupling, DGSs can also be used for bandwidth enhancement and impedance matching.

Iterative methods are often employed in designing DGSs and antennas in general. Metaheuristic algorithms are widely used because of lower relative computational cost and their ability to avoid local optima. Some metaheuristics that have been deployed in the design of antennas include Particle Swarm Optimizer (PSO) in [1-4], Invasive Weed Optimizer (IWO) in [5-7], Salp Swarm Algorithm (SSA) in [8] and Quasi-Opposition-based Grey Wolf Optimizer (QOGWO) in [9]. Among these, the Grey Wolf Optimizer (GWO) has received particular attention for electromagnetic optimization problems.

The GWO's performance was investigated in [10], where it was successfully used to synthesize an array, design an E-shaped microstrip antenna, and design a microstrip dipole. It was found to perform well compared with other metaheuristics

and is therefore suitable for electromagnetic optimization problems.

Metaheuristic algorithms often face a tradeoff between exploration and intensification, favoring one over the other. Furthermore, optimization algorithms perform differently on different types of problems: an optimizer that performs well on one problem may perform poorly on another. To improve performance, an optimizer can be hybridized with another metaheuristic whose strengths complement its own. Various improvements have been made on existing metaheuristic optimization algorithms. For instance, in [11], crossover and mutation operators, typical in Genetic Algorithms (GAs), were used to improve the search diversity of the cuckoo search algorithm. In [12], the Harris Hawks Algorithm (HHA) was improved by adopting Opposition-Based Learning (OBL), Lévy flight and chaotic logistic map.

The GWO may sometimes converge prematurely. This problem has been addressed in literature such as [13] and [14], where the parameter a in the original GWO, which governs the transition from the exploration phase to exploitation phase by decreasing linearly from 2 to 0, is modified to be non-linear. Hybridization with another optimizer can also improve the accuracy of the GWO, as demonstrated in [15], where the hybrid Jaya-GWO was used to design an antenna for application in 5G devices. Two E-shaped antennas were used to test the algorithm, the first operating at 3.7 GHz and the second at 26 GHz.

The GWO was originally introduced in [16], and OBL was introduced in [17]. Quasi-oppositional learning, an improvement on OBL, was introduced in [18], where randomness was introduced into the selection of the opposite solution. In [19], the dimensional diversity metric was introduced and later used in [20] to develop operators for managing population in a way that avoids stagnation while enhancing exploitation efficiency. These operators were applied to differential evolution.

Several antenna designs have been proposed in literature. In [21], a four-element coplanar waveguide monopole was designed to operate at 3.5 GHz, whereas in [22], a four-element tri-band meander-line antenna with a partial ground was designed. Unlike these designs, our proposed antenna uses a full ground plane for easier embedding with other components on a PCB. In [23-25], a base rectangular patch design is used, after which DGSs and slots of various shapes are introduced to enhance antenna performance, whereas in [26], slots are introduced on a rectangular patch to enhance bandwidth and efficiency. In [27], slots are loaded onto various microstrip patch shapes to enhance their performance. In two of the antenna elements of the design proposed in [25], top corner slots are introduced on the radiator. Each element has a square DGS on the ground plane to reduce coupling between MIMO elements. Rectangular parasitic elements are also placed between the antenna elements to reduce coupling. In contrast, our proposed design features a rectangular patch with corner slots and an L-shaped parasitic element, which affects the resonant behavior of the antenna. Impedance matching is further improved using a non-uniform inverted U-shaped DGS.

In this study, we use an Efficient Quasi-Oppositional Grey Wolf Optimizer (EQOGWO), which serves the dual purpose of improving the rate of convergence and avoiding premature convergence by considering population diversity when determining whether to evaluate the opposite solutions. The optimizer is used to design a compact dual-band antenna comprising an inverted U-shaped DGS, square slots, and an L-shaped parasitic element.

The main contributions of this study are:

- A novel design of a compact dual-band antenna comprising an inverted U-shaped DGS, square slots, and an L-shaped parasitic element.
- An efficient version of the QOGWO for iterative DGS design.

II. ANTENNA DESIGN METHODOLOGY

This work follows an iterative design approach, where the geometry of the antenna evolved over different stages. First, a rectangular microstrip patch was designed using established formulations for operation at the first frequency of interest. Slots and a parasitic element were then introduced, leading to the introduction of the second resonance mode. Finally, a DGS was introduced on the ground plane to achieve dual-band matching. This process is summarized in Figure 1.

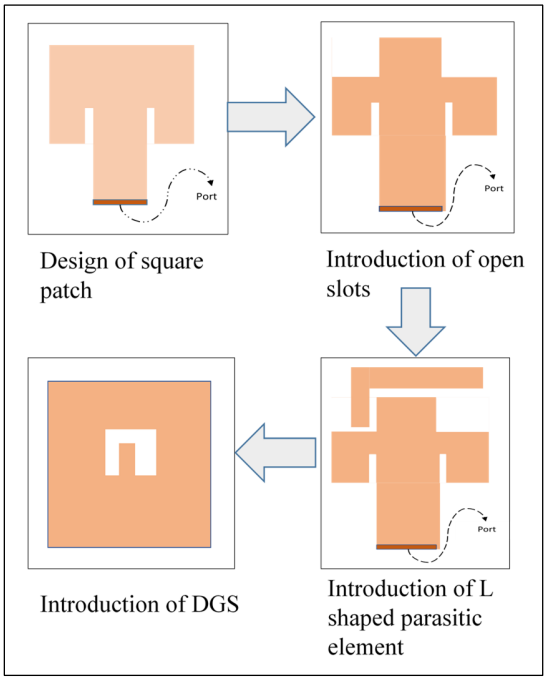

Fig. 1. Design stages of the proposed dual-band microstrip antenna.

To optimize the radiating structure for dual-band operation, to position the DGS appropriately, and to determine the correct dimensions for the different DGS sections, this work relied on the EQOGWO. The optimization algorithm was implemented in MATLAB, whereas Ansys HFSS was used as the electromagnetic solver. To evaluate the fitness of each solution,

the algorithm in MATLAB was interfaced with the HFSS simulator so that, at every iteration, the antenna DGS parameters in the simulator were updated and antenna performance evaluated. The optimization process is as depicted in Figure 2.

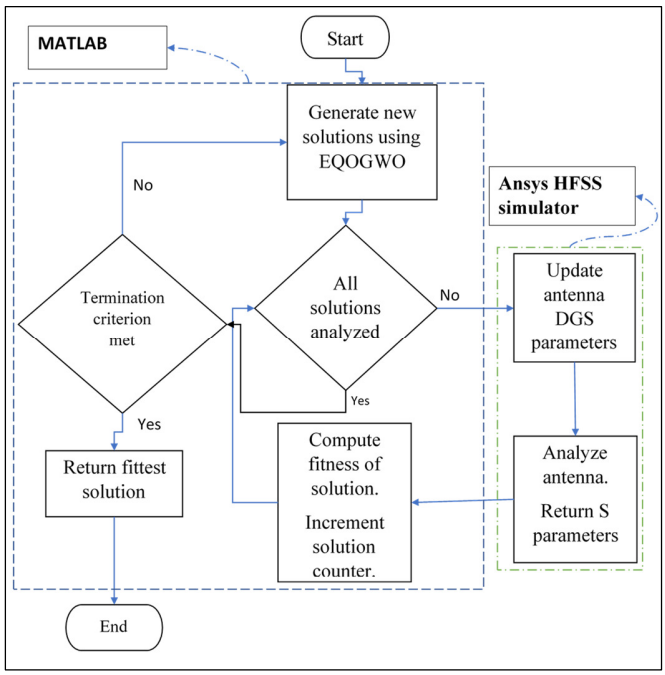

Fig. 2. Flow chart of the antenna optimization process.

A. Antenna Geometry

The different stages of the design are described in the following sections. The setup uses an FR4 substrate of 60 mm × 60 mm × 6 mm and a ground plane of 60 mm × 60 mm. The transmission line model was used to design the initial patch using (1)–(4), elaborated in [28].

1) Rectangular Patch

The following procedure was used to obtain the initial rectangular patch:

- The initial width was determined using (1):

$$W = \frac{C_0}{2f_r}\sqrt{\frac{2}{\varepsilon_r+1}} \quad (1)$$

where C_0 represents the speed of light in free space, f_r represents the center frequency, and ε_r represents the dielectric constant.

- The effective dielectric constant was determined using (2):

$$\varepsilon_{reff} = \frac{\varepsilon_r+1}{2} + \frac{\varepsilon_r-1}{2}\left[1+12\frac{h}{W}\right]^{-\frac{1}{2}},\ {}^{W}/_{h} > 1 \quad (2)$$

where h is the height or thickness of the substrate, W is the width of the patch, and ε_{reff} is the effective dielectric constant.

- The change in electric length as a result of fringing was determined using (3):

$$\frac{\Delta L}{h} = 0.412\frac{(\varepsilon_{reff}+0.3)\left(\frac{W}{h}+0.264\right)}{(\varepsilon_{reff}-0.258)\left(\frac{W}{h}+0.8\right)} \quad (3)$$

where ΔL represents the change in electric length.

- The patch length was then determined using (4).

$$L = \frac{C_O}{2f_r\sqrt{\varepsilon_{reff}}} - 2\Delta L \quad (4)$$

where L is the length of the patch.

- The final values for width and length were obtained through optimization.

2) Symmetrical Open Slots

Symmetrical slots were cut on the top corners of the rectangular patch. The slot length L_n, was chosen such that $L_n < L_r - L_s$, where L_r is the length of the initial patch and L_s is the length of the feed-point slot. A parameter sweep of L_n was performed to identify a length that lowers the operating frequency, indicating miniaturization of the patch resonance. After this step, L_r and W_r (the length and width of the initial patch) were further optimized to maintain the second resonance at 3.5 GHz.

3) Parasitic Element

A quarter-wave L-shaped parasitic element was introduced, and its parameters were optimized so that the antenna achieves dual-band operation at 2.6 GHz and 3.5 GHz.

4) Defected Ground Structure

The DGS was designed iteratively using the procedure summarized in Figure 2. The EQOGWO was implemented using MATLAB. To evaluate the fitness of each solution, the algorithm in MATLAB was interfaced with the Ansys HFSS simulator, so that for every iteration, the DGS parameters in the simulator were updated and the antenna performance evaluated. The S-parameter data were then passed back to the optimizer.

The objective function was defined as:

$$f = S_{11}(3.5\ \text{GHz}) + 10 \times |\min(|S_{11}(2.6\ \text{GHz})| - 18, 0)| \quad (5)$$

where $S_{11}(2.6\ \text{GHz})$ and $S_{11}(3.5\ \text{GHz})$ represent the S-parameters at 2.6 GHz and 3.5 GHz, respectively. The parameter limits for the optimizations are given in Table I.

TABLE I. PARAMETER LIMITS FOR DGS OPTIMIZATION

Parameter	Range (mm)
L_1	5–15
W_1	2–6
L_2	2–16
W_2	2–5
W_3	2–6
X_p	20–40
Y_p	16–20

III. OPTIMIZATION ALGORITHM

The proposed algorithm is driven by two key ideas:

- Evaluation of the opposite of a candidate solution when the likelihood that it will be fitter is high, leading to a more efficient search.
- Evaluation of the opposite of a candidate solution when there is a high likelihood of premature convergence, leading to local optima avoidance.

The initial set of solutions is generated using Latin Hypercube Sampling (LHS) to ensure a diverse initial population and to provide a good initial value for diversity. The pseudo code for the proposed EQOGWO is as described below.

```
EQOGWO pseudo code
Initialize population of candidate
solutions using LHS.
Initialize GWO parameters and set Maximum
Diversity to 0.
While termination criterion not met:
   Compute Diversity using (13);
   If Diversity > Maximum Diversity:
      Make Diversity the new Maximum
      Diversity;
   End if
   If random [0,1] > (1 - Diversity/Maximum
   Diversity) and random [0,1] > (1-Current
   Iteration/Max Iterations):
      Evaluate fitness of each candidate
      solution;
      Set Alpha, Beta, Delta using the
      respective three best solutions;
   Else
      Evaluate fitness of each candidate
      solution and its quasi-oppositional
      point;
      Replace candidate solution with its
      opposite if the opposite is better;
      Set Alpha, Beta, Delta using the
      respective three best solutions;
   End if
   Determine next candidate solution using
   GWO movement equations;
   Increase iteration count;
End while
```

In the algorithm, the probability that the opposite point will be evaluated, i.e. the jumping rate, is determined by relative diversity and the phase of the optimization process, as determined by Current Iteration and Maximum Iterations. The rationale here is that the combination of relative diversity and the ratio of Current Iteration to Maximum Iterations provides an estimate of premature convergence, indicating when the opposite point could yield a fitter solution.

Some key ideas from literature that have been incorporated into the algorithm are described in the remainder of this section.

A. Grey Wolf Optimizer

In the GWO, the movement of search agents, or wolves, is governed by (6)–(9), which are defined and explained in [16] as follows:

$$\vec{D} = |\vec{C}.\vec{X}_P(t) - \vec{X}(t)| \quad (6)$$

where $\vec{D}$ represents the distance between the wolves and the prey, $\vec{C}$ represents a coefficient vector, $\vec{X}_P$ represents the position vector of the target, and $\vec{X}$ represents the position of the wolves.

$$\vec{X}(t+1) = \vec{X}_p(t) - \vec{A}.\vec{D} \quad (7)$$

where $\vec{X}(t+1)$ represents the next position of the wolves, and $\vec{A}$ is a coefficient vector.

$$\vec{A} = 2\vec{a}.\vec{r}_1 - \vec{a} \quad (8)$$

$$\vec{C} = 2.\vec{r}_2 \quad (9)$$

where $\vec{r}_1$ and $\vec{r}_2$ are random vectors that range between 0 and 1, and $\vec{a}$ is initialized with a value of 2 and gradually reduced to 0. To implement the GWO, $\vec{X}_P$ is replaced by Alpha, Beta, and Delta, which are the three best candidate solutions at different instances. The final solution is obtained by averaging the three results.

B. Opposition-Based Learning and Quasi-Opposition-Based Learning

The opposite point is defined in [17] as:

$$\tilde{x} = u + l - x \quad (10)$$

where $\tilde{x}$ represents the opposite of x, u is the upper bound, and l is the lower bound.

The quasi-oppositional point, which introduces randomness into the selection of the opposite solution, is defined in [18] as:

$$y \in \left(\frac{u+l}{2}, \tilde{x}\right) \quad (11)$$

where y is a random variable representing the quasi-oppositional point.

C. Diversity

In [19], the dimensional diversity metric is defined as:

$$\mathrm{Div}_j = \frac{1}{n}\sum_{i=1}^{n}\left|\mathrm{median}(x_j) - x_{ij}\right| \quad (12)$$

$$\mathrm{Div} = \frac{1}{m}\sum_{j=1}^{m}\mathrm{Div}_j \quad (13)$$

where x_{ij} is the value of dimension j of search agent i, n is the population of search agents, $\mathrm{median}(x_j)$ is the median value in dimension j, and m is the number of dimensions.

IV. PERFORMANCE OF THE OPTIMIZATION ALGORITHM

To evaluate the performance of the EQOGWO, common benchmark functions listed in Table II were used. Its average performance on each function was compared with PSO, IWO, Intelligent Grey Wolf Optimizer (IGWO), GWO, and

QOGWO, with jumping rates set at $jr = 0.3$ and $jr = 0.6$. The functions in Table II vary in terms of modality and can therefore be used to assess different properties of metaheuristic algorithms, such as exploration ability, exploitation capability, and ability to avoid local optima. Functions F1–F7 are unimodal and provide information on the algorithm's exploitation capability, whereas functions F8–F13 are multimodal and offer insight into the algorithm's exploration capabilities. They have been used in literature such as [16] to evaluate performance of metaheuristic algorithms.

The evaluation was conducted using the following parameters:

- Maximum of 500 iterations for each trial, except for EQOGWO and QOGWO, where the maximum iterations were 250.
- 50 independent trials for each objective function,
- Maximum of 100 search agents for each optimization algorithm.

The average score of each algorithm on the benchmark functions is reported in Tables III–VI. Performance ranking was performed using the Friedman test and tabulated in Tables VII–X.

TABLE II. BENCHMARK FUNCTIONS USED FOR OPTIMIZER EVALUATION

Function	Formula	Dimension	Range	Function minima
F1,Sphere	$\sum_{i=1}^{n} x_i^2$	30	[-100, 100]	0
F2, Schwefel	$\sum_{i=1}^{n} \lvert x_i \rvert + \prod_{i=1}^{n} \lvert x_i \rvert$	30	[-10, 10]	0
F3, Schwefel	$\sum_{i=0}^{n-1} \{\sum_{j=0}^{j<i} x_i\}^2$	30	[-100, 100]	0
F4, Schwefel	$max_i\{x_i, 1 \le i \le n\}$	30	[-100, 100]	0
F5, Generalized Rosenbrock	$\sum_{i=1}^{n-1}[100\ (x_{1+1} - x_i^2)^2 + (x_i - 1)^2]$	30	[-30, 30]	0
F6, Step	$\sum_{i=1}^{n}(x_i + 0.5)^2$	30	[-100, 100]	0
F7, Quartic	$\sum_{i=1}^{n} ix_i^4 + random[0,1)$	30	[-1.28, 1.28]	0
F8, Generalized Schwefel	$\sum_{i=1}^{n} -xisin(\sqrt{\lvert x_i \rvert})$	30	[-500, 500]	-418.9829
F9, Rastrigin	$\sum_{i=1}^{n}[x_i^2 - 10cos(2\pi x_i) + 10]$	30	[-5.12, 5.12]	0
F10, Ackley	$-20exp\left(-0.2\sqrt{\frac{1}{n}\sum_{i=1}^{n} x_i^2}\right) - exp\left(\frac{1}{n}\sum_{i=1}^{n} cos(2\pi x_i)\right)$	30	[-32, 32]	0
F11, Griewank	$\frac{1}{4000}\sum_{i=1}^{n} x_i^2 - \prod_{i=1}^{n} \cos\left(\frac{x_i}{\sqrt{i}}\right) + 1$	30	[-600, 600]	0
F12, Generalized penalized	$\frac{\pi}{n}\{10\sin(\pi y_1) + \sum_{i=1}^{n-1}(y_i - 1)^2\ [1 + 10sin^2(\pi y_{1+1})] + (y_n - 1)^2\} + \sum_{i=1}^{n} u(x_i, 10,100,4)$, $y_i = 1 + \frac{x_i+1}{4}$, $u(x_i, a, k, m) = \begin{cases} k(x_i - a)^m & x_i > a \\ 0 & -a < x_i < 1 \\ k(-x_i - a)^m & x_i < -a \end{cases}$	30	[-50, 50]	0
F13	$0.1\{sin^2(3\pi x_1) + \sum_{i=1}^{n}(x_i - 1)^2\ [1 + sin^2(3\pi x_i + 1)] + (x_n - 1)^2[1 + sin^2(2\pi x_n)]\} + \sum_{i=1}^{n} u(x_i, 5,100,4)$	30	[-50, 50]	0

TABLE III. PERFORMANCE OF ALGORITHMS ON UNIMODAL BENCHMARK FUNCTIONS (FITNESS VALUES)

Function	GWO	IWO	PSO	EQOGWO (250 iterations)	IGWO	QOGWO (250 iterations, $jr = 0.3$)	QOGWO (250 iterations, $jr = 0.6$)
F1	5.11E-41	2.16E+04	6.37E-31	4.21E-105	1.90E-38	1.41E-65	1.43E-124
F2	5.71E-24	0.046	1.61E-05	1.23E-55	1.88E-22	3.52E-37	1.46E-67
F3	5.76E-12	3.03E+04	1.4875	1.97E-82	5.03E-10	2.08E-47	8.95E-102
F4	2.07E-10	52.6592	0.1309	1.47E-45	2.41E-10	1.64E-27	3.84E-57
F5	26.52366	292.8737	33.174	26.77558444	26.27226418	26.5921874	26.66786388
F6	0.175478	2.08E+04	1.07E-30	0.492735809	0.142473393	0.346033459	0.38557141
F7	0.000553	0.0251	0.009	3.68E-05	0.000506802	3.59E-05	3.61E-05

TABLE IV. PERFORMANCE OF ALGORITHMS ON MULTIMODAL BENCHMARK FUNCTIONS (FITNESS VALUES)

Function	GWO	IWO	PSO	EQOGWO (250 iterations)	IGWO	QOGWO (250 iterations, $jr = 0.3$)	QOGWO (250 iterations, $jr = 0.6$)
F8	-6485.51	-5.00E+03	-6.89E+03	-5373.22498	-6042.693347	4.63E-05	3.22E-05
F9	0.829156	57.4648	45.4497	0	0.399523619	0	0
F10	2.71E-14	18.9865	0.3678	2.38E-15	2.29E-14	2.95E-15	3.16E-15
F11	0.002528	585.2326	0.0106	0	0.000695076	0	0
F12	0.01656	38.3626	0.0436	0.024157791	0.014152909	0.025972166	0.026559906
F13	0.187988	3.59E+04	0.0044	0.469542436	0.159633587	0.279378168	0.354853232

TABLE V. AVERAGE NUMBER OF EVALUATIONS REQUIRED FOR CONVERGENCE ON UNIMODAL FUNCTIONS

Function	GWO	EQOGWO (250 iterations)	IGWO	QOGWO (250 iterations, $jr = 0.3$)	QOGWO (250 iterations, $jr = 0.6$)
F1	49900	37540	49900	32466	39918
F2	49900	37260	49900	32118	39792
F3	49900	37376	49898	32522	39826
F4	49900	37382	49900	32306	39892
F5	49892	37628	49896	32188	39942
F6	49900	37540	49896	32316	39980
F7	37738	20810	38862	19538	22936

TABLE VI. AVERAGE NUMBER OF EVALUATIONS REQUIRED FOR CONVERGENCE ON MULTIMODAL FUNCTIONS

Function	GWO	EQOGWO (250 iterations)	IGWO	QOGWO (250 iterations, $jr = 0.3$)	QOGWO (250 iterations, $jr = 0.6$)
F8	49544	30540	46596	21192	21340
F9	23900	4642	21460	6832	5442
F10	21122	11398	21322	12848	11804
F11	17312	5298	16418	7474	6064
F12	49898	37408	49898	32404	39962
F13	49894	37422	49900	3.24E+04	39796

TABLE VII. MEAN FITNESS RANK OF ALGORITHMS IN UNIMODAL FUNCTIONS

Algorithm	Mean rank
GWO	3.7143
IWO	7
PSO	5.2857
EQOGWO	3.1429
IGWO	3.8571
QOGWO (250 iterations, $jr = 0.3$)	2.8571
QOGWO (250 iterations, $jr = 0.6$)	2.1429
P-value	0.00044692

TABLE VIII. MEAN FITNESS RANK OF ALGORITHMS IN MULTIMODAL FUNCTIONS

Algorithm	Mean rank
GWO	3.6667
IWO	6.6667
PSO	4.3333
EQOGWO	3
IGWO	3
QOGWO (250 iterations, $jr = 0.3$)	3.5
QOGWO (250 iterations, $jr = 0.6$)	3.8333
P-value	0.048791

TABLE IX. MEAN RANK OF ALGORITHMS BASED ON NUMBER OF EVALUATIONS ON UNIMODAL FUNCTIONS

Algorithm	Mean rank
GWO	4.5
EQOGWO	2
IGWO	4.5
QOGWO (250 iterations, $jr = 0.3$)	1
QOGWO (250 iterations, $jr = 0.6$)	3
P-value	1.826E-05

TABLE X. MEAN RANK OF ALGORITHMS BASED ON NUMBER OF EVALUATIONS ON MULTIMODAL FUNCTIONS

Algorithm	Mean rank
GWO	4.5833
EQOGWO	1.6667
IGWO	4.4167
QOGWO (250 iterations, $jr = 0.3$)	2
QOGWO (250 iterations, $jr = 0.6$)	2.3333
P-value	0.00089091

The algorithm rankings are summarized below:

- Mean fitness rank in unimodal functions (Table VII): EQOGWO achieved the third-best ranking, after QOGWO with jr =0.6 and QOGWO with jr =0.3.
- Mean fitness rank in multimodal functions (Table VIII): EQOGWO achieved the best performance, alongside IGWO.
- Mean rank based on evaluations required to converge in unimodal functions (Table IX): EQOGWO achieved the second-best performance after QOGWO with $jr = 0.3$.
- Mean rank based on evaluations required to converge in multimodal functions (Table X): EQOGWO achieved the best performance.

Based on these findings, we conclude that the best application of the EQOGWO is in multimodal optimization problems. However, we observed that it still outperforms the original GWO and IGWO in unimodal optimization problems. Therefore, for black box optimization problems with unknown fitness landscapes, EQOGWO is a strong choice.

In this study, we consider the antenna optimization problem as a black box optimization problem with an unknown fitness landscape, making EQOGWO well-suited for the task.

V. ANTENNA PERFORMANCE

The antenna was designed in four stages, with each geometry iteration aimed at improving the dual-band performance of the overall structure at 2.6 GHz and 3.5 GHz.

A. Single Antenna

1) Rectangular Patch

The rectangular patch was designed using (1)–(4). The resultant structure is shown in Figure 3, and the corresponding dimensions are tabulated in Table XI. The S-parameter plot is illustrated in Figure 4.

TABLE XI. DIMENSIONS OF THE RECTANGULAR PATCH

Parameter	Value (mm)
L_r	20
W_r	28
L_s	6
W_s	1
L_f	22.353
W_f	11.5

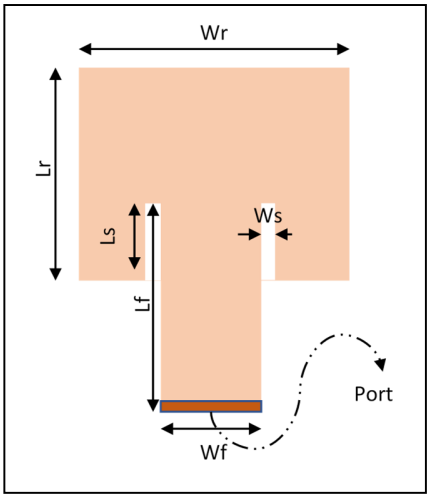

Fig. 3. Geometry of initial rectangular patch.

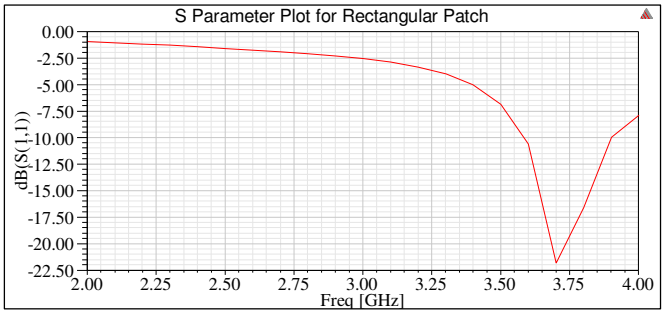

Fig. 4. S_{11} plot of the initial rectangular patch.

2) Patch with Open Square Slots

When open slots were introduced into the rectangular patch and the structure was optimized to operate at 3.5 GHz, the resultant geometry was as shown in Figure 5 and the dimensions were as tabulated in Table XII. The S-parameter behavior is illustrated in Figure 6.

TABLE XII. DIMENSIONS OF THE RECTANGULAR PATCH WITH SLOTS

Parameter	Value (mm)
L_r	18
W_r	26
L_s	6
W_s	1
L_f	22.353
W_f	11.5
L_n	6.9437

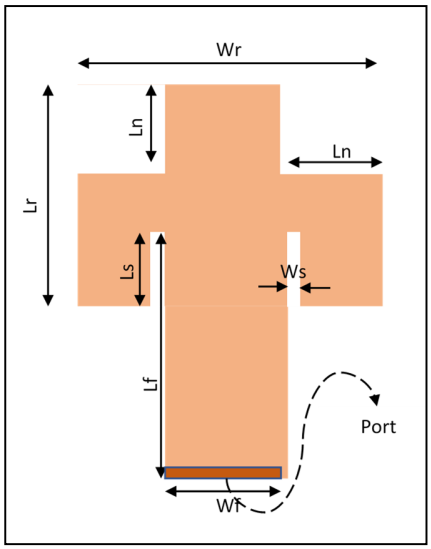

Fig. 5. Geometry of patch with slots.

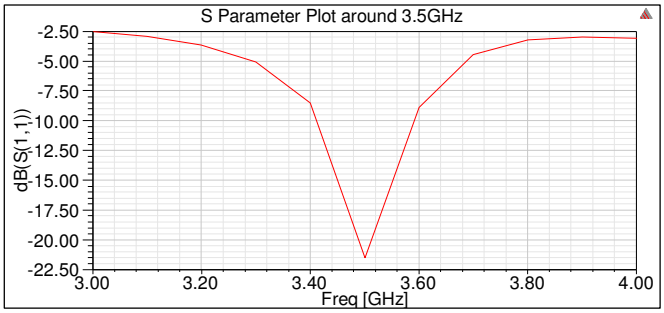

Fig. 6. S_{11} plot of the patch with slots.

Introducing the open slots resulted in a lower return loss at 3.5GHz. Miniaturization was also achieved, as indicated by the values of L_r and W_r. This is because the slots lengthen the current path leading to the lowering of the resonant frequency when everything else remains unchanged.

3) Patch with Open Square Slots and L-Shaped Parasitic Element

When the L-shaped parasitic element was introduced to the slotted patch, the resultant geometry was as shown in Figure 7, and the corresponding dimensions are tabulated in Table XIII. The S-parameter behavior is illustrated in Figure 8.

TABLE XIII. DIMENSIONS OF PATCH WITH SLOTS AND PARASITIC ELEMENT

Parameter	Value (mm)
L_r	18
W_r	26
L_s	6
W_s	1
L_n	6.9437
L_p	9
W_p	3.8
L_{p2}	22
L_f	22.353
W_f	11.5
W_{p2}	5
g	1

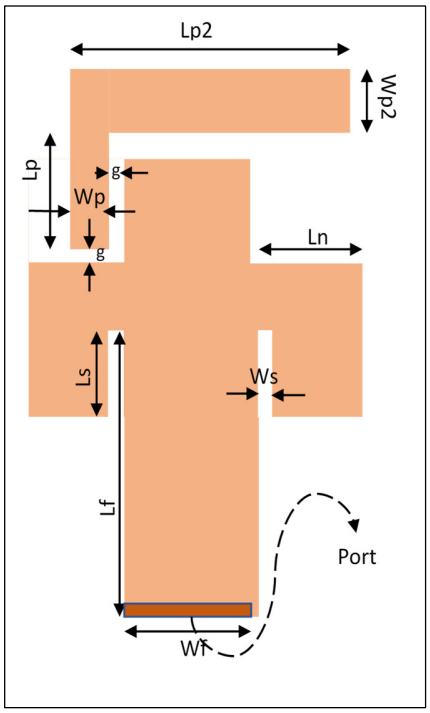

Fig. 7. Geometry of patch with slots and parasitic element.

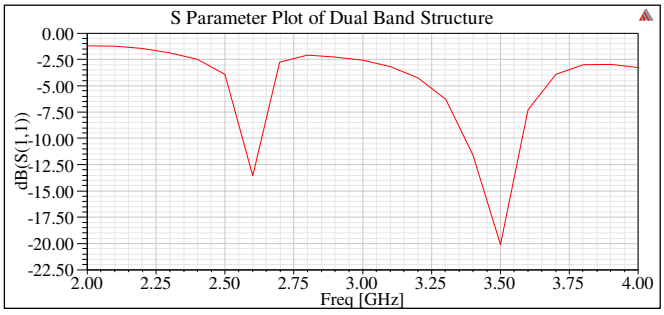

Fig. 8. S_{11} plot of the patch with slots and parasitic element.

As observed from the S-parameter plot in Figure 8, introducing the L-shaped parasitic element introduces an additional resonant mode at 2.6 GHz. This new resonant mode requires further matching.

4) Introduction of a Folded Defected Ground Structure

When the DGS, whose geometry is shown in Figure 9, was introduced on the ground plane and optimized for operation at 2.6 GHz and 3.5 GHz, the resultant dimensions were as tabulated in Table XIV. The S-parameter behavior was as shown in Figures 10 and 11.

TABLE XIV. DIMENSIONS OF THE DGS OBTAINED USING EQOGWO

Parameter	Value (mm)
L_1	13.15757
W_1	4.654382
L_2	2
W_2	4.88364
W_3	2.342865
X_p	32.00553
Y_p	18.95985

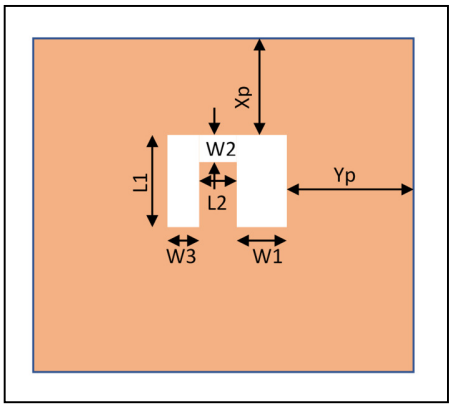

Fig. 9. Ground plane with DGS.

Figure 10 shows that when the non-uniform inverted U-shaped (DGS) is introduced, the S_{11} value at 2.6 GHz is reduced to −20dB. This redaction indicates that the incorporation of the DGS effectively enhances the impedance matching of the antenna at 2.6 GHz, leading to improved overall performance.

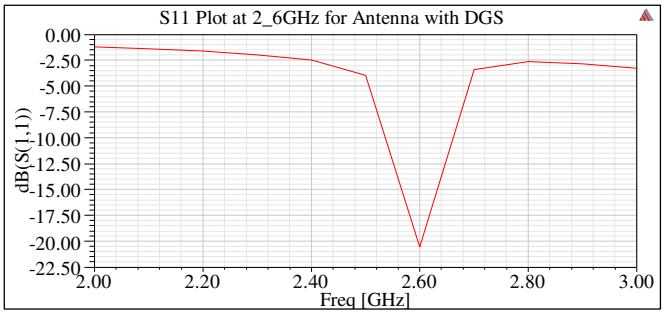

Fig. 10. S_{11} plot at 2.6 GHz with DGS introduced.

Figure 11 shows that the S11 value at 3.5 GHz decreases further when the DGS is introduced. This reduction demonstrates that the incorporation of the DGS effectively enhances the impedance matching of the antenna at 3.5 GHz.

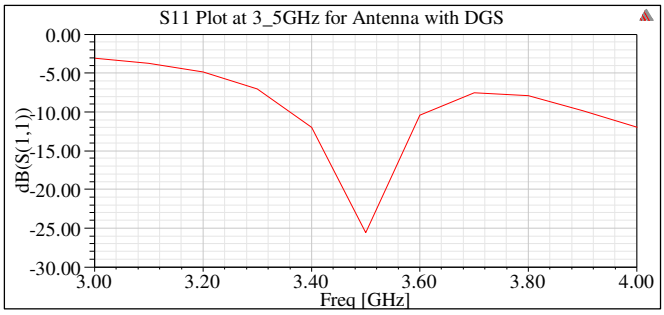

Fig. 11. S_{11} plot at 3.5 GHz with DGS introduced.

When the EQOGWO was used to optimize the antenna, a simulated S_{11} value of −20.4 dB at 2.6 GHz and −25.69 dB at 3.5 GHz was achieved in 9 iterations and 96 full-wave evaluations. For comparison, the original GWO achieved an S_{11} value of −19.1686 dB at 2.6 GHz and −14.0674 dB at 3.5 GHz in 23 iterations and 138 evaluations. The EQOGWO therefore led to a more efficient optimization process, requiring fewer full-wave evaluations. The convergence curve in Figure 12 shows a comparison between the antenna optimization using EQOGWO and GWO. The fitness was computed using (5).

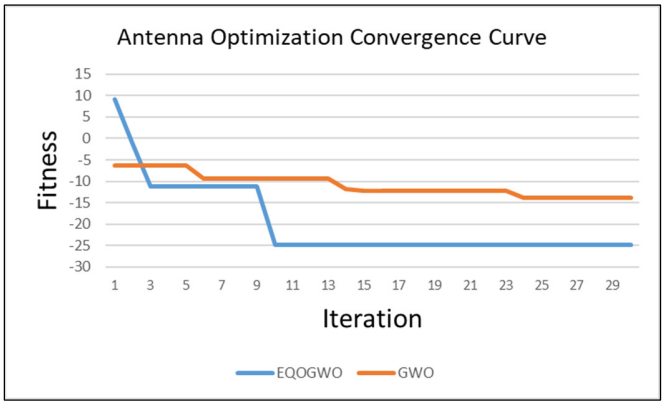

Fig. 12. Convergence curves for single-element antenna optimization.

B. *Two-Element Antenna Structure*

A two-element configuration was also modeled in HFSS, as shown in Figure 13, with the edge-to-edge distance between the first and second antennas being 4 mm.

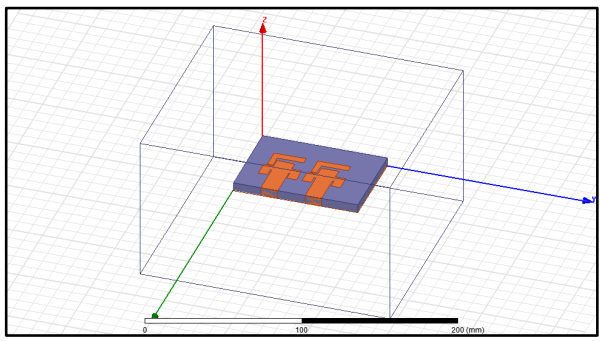

Fig. 13. Two closely arranged antennas.

1) *Operation at 2.6 GHz*

Figure 14 shows that when two antennas of the proposed structure without DGS are closely placed, S_{11} at 2.6 GHz is affected and goes above the desired maximum value of -10 dB, indicating increased impedance mismatch.

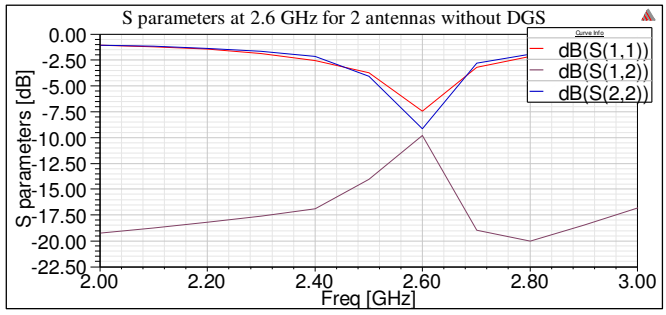

Fig. 14. S-parameters around 2.6 GHz without DGS.

Figure 15 shows that introducing the DGS lowers S_{11} below -10 dB, improving matching.

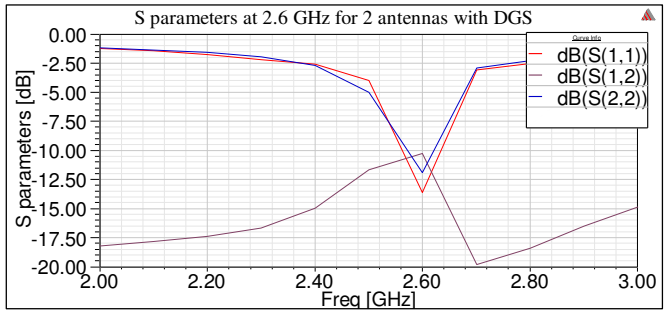

Fig. 15. S-parameters around 2.6 GHz with DGS introduced.

2) *Operation at 3.5 GHz*

Figure 16 shows that when two antennas of the proposed structure without DGS are closely arranged, S_{11} at 3.5 GHz is affected but does not go above −10 dB.

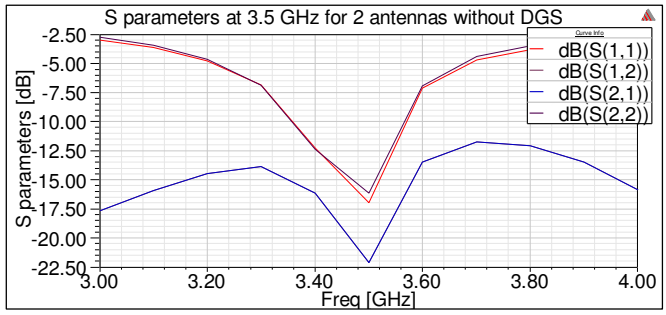

Fig. 16. S-parameters around 3.5 GHz without DGS.

Figure 17 shows that introducing the inverted U-shaped DGS results in improved impedance matching at 3.5 GHz, confirming the effectiveness of the proposed antenna design.

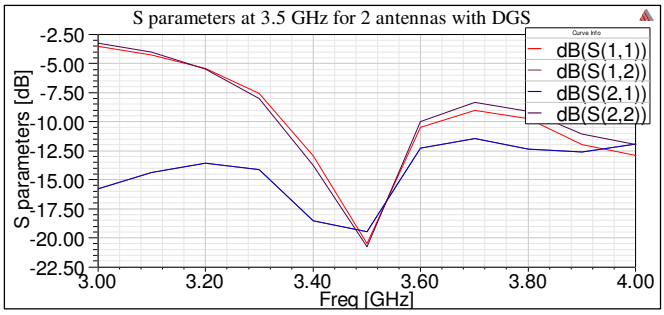

Fig. 17. S-parameters around 3.5 GHz with DGS introduced.

Table XV compares the structure, footprint, and S_{11} performance of our design with recent related work.

TABLE XV. COMPARISON OF THE PROPOSED ANTENNA WITH RELATED WORK

Ref	Structure	Size of single radiating element (mm)	Freq. (GHz)	S_{11} (dB)
[23]	Rectangular patch with L slot and DGS	47.74 × 69.77	2.7	−23.5
[24]	Rectangular patch with U-shaped DGS	14.5 × 38.22	2.4	−26.88
[25]	Rectangular patch with slots, rectangular DGS, and rectangular parasitic elements	11.38 × 11.38	6	< −10
Proposed design	Slotted rectangular patch with L parasitic element and DGS	42.4 × 26	2.6, 3.5	−20, −25

Similar to our approach, in both [23] and [24], the initial design is a rectangular microstrip antenna, with DGS and slots of various shapes used to enhance antenna performance. These designs are well matched at 2.7 GHz and 2.4 GHz, respectively. Our proposed design on the other hand is dual-band, operating at 2.6 GHz and 3.5 GHz. The footprint of our structure is smaller than that in [23] but larger than that in [24] due to the additional resonant mode achieved using the L parasitic element. The structures proposed in [25] have smaller footprints because of the higher operating frequency.

In summary, introducing open slots onto the rectangular patch lengthens the current path, lowering the resonant frequency, which can also be interpreted as miniaturization. The quarter-wave L-shaped parasitic element resonates at 2.6 GHz, introducing a second resonant mode, as seen in Figure 8. The objective function in (5) used to iteratively design the inverted U-shaped DGS ensures impedance matching at 2.6 GHz without causing mismatch at 3.5 GHz, explaining the observations in Figures 10 and 11. Placing two antennas close to each other, as in Figure, causes impedance mismatch due to coupling via surface waves. Without the DGS, the reflections caused by the mismatch raises the S-parameters above the desired maximum limit (Figure 14). With the DGS introduced, there is improved matching and the S-parameters are at the desired levels (Figures 15 and 17).

VI. CONCLUSION AND FUTURE WORK

In this study, a non-uniform inverted U-shaped Defected Ground Structure (DGS) and an Efficient Quasi-Oppositional Grey Wolf Optimizer (EQOGWO) were used to design and optimize a compact dual-band antenna operating at 2.6 GHz and 3.5 GHz. The dimensional diversity metric was employed to dynamically determine the QOGWO's jumping rate, improving the efficiency of the optimization process. The antenna was simulated using Ansys HFSS, a Finite Element Method (FEM)-based electromagnetic solver. The designed antenna attained a simulated S_{11} value of −20 dB at 2.6 GHz and −25.69 dB at 3.5GHz, meeting the target of a maximum of −10 dB within the operating frequency ranges. Compared to the Grey Wolf Optimizer (GWO), the EQOGWO achieved comparable or better results with fewer evaluations for both benchmark functions and the antenna optimization problem.

A limitation of the iterative approach used to design the DGS-based antenna is that, for more complicated structures, full-wave evaluations can become even more computationally expensive. In future work, an analytical approach that provides physical insight may be incorporated to make the design process more intuitive and efficient, for example, when designing additional DGS-based decoupling structures for multi-element antennas.

REFERENCES

[1] N. Jin and Y. Rahmat-Samii, "Particle Swarm Optimization for Antenna Designs in Engineering Electromagnetics," *Journal of Artificial Evolution and Applications*, vol. 2008, no. 1, Mar. 2008, Art. no. 728929, https://doi.org/10.1155/2008/728929.

[2] N. Jin and Y. Rahmat-Samii, "Advances in Particle Swarm Optimization for Antenna Designs: Real-Number, Binary, Single-Objective and Multiobjective Implementations," *IEEE Transactions on Antennas and Propagation*, vol. 55, no. 3, pp. 556–567, Mar. 2007, https://doi.org/10.1109/TAP.2007.891552.

[3] M. T. Islam, N. Misran, T. C. Take, and Mohd. Moniruzzaman, "Optimization of microstrip patch antenna using Particle swarm optimization with curve fitting," in *2009 International Conference on Electrical Engineering and Informatics*, Bangi, Malaysia, 2009, pp. 711–714, https://doi.org/10.1109/ICEEI.2009.5254724.

[4] M. M. Khodier and C. G. Christodoulou, "Linear array geometry synthesis with minimum sidelobe level and null control using particle swarm optimization," *IEEE Transactions on Antennas and Propagation*, vol. 53, no. 8, pp. 2674–2679, Aug. 2005, https://doi.org/10.1109/TAP.2005.851762.

[5] M. B. Saleh, E. A. Doumith, and R. Sarkis, "Invasive Weed Optimization for Antenna Design: Case of 4G/5G Multi-band Antenna," in *2020 IEEE International Symposium on Antennas and Propagation and North American Radio Science Meeting*, Montreal, Canada, 2020, pp. 2071–2072, https://doi.org/10.1109/IEEECONF35879.2020.9330238.

[6] S. Karimkashi and A. A. Kishk, "Invasive Weed Optimization and its Features in Electromagnetics," *IEEE Transactions on Antennas and Propagation*, vol. 58, no. 4, pp. 1269–1278, Apr. 2010, https://doi.org/10.1109/TAP.2010.2041163.

[7] S. H. Sedighy, A. R. Mallahzadeh, M. Soleimani, and J. Rashed-Mohassel, "Optimization of Printed Yagi Antenna Using Invasive Weed Optimization (IWO)," *IEEE Antennas and Wireless Propagation Letters*, vol. 9, pp. 1275–1278, 2010, https://doi.org/10.1109/LAWP.2011.2105458.

[8] A. D. Boursianis, S. K. Goudos, T. V. Yioultsis, K. Siakavara, and P. Rocca, "MIMO Antenna Design for 5G Communication Systems Using Salp Swarm Algorithm," in *2020 International Workshop on Antenna*

Technology, Bucharest, Romania, 2020, pp. 1–3, https://doi.org/10.1109/iWAT48004.2020.1570618331.

[9] H.-Y. Zhu, W.-D. Li, and H.-Y. Zhao, "Antenna Optimization Based on Quasi-Opposition Grey Wolf Optimization Algorithm," in *2022 International Conference on Microwave and Millimeter Wave Technology*, Harbin, China, 2022, pp. 1–3, https://doi.org/10.1109/ICMMT55580.2022.10022853.

[10] X. Li and K. M. Luk, "The Grey Wolf Optimizer and Its Applications in Electromagnetics," *IEEE Transactions on Antennas and Propagation*, vol. 68, no. 3, pp. 2186–2197, Mar. 2020, https://doi.org/10.1109/TAP.2019.2938703.

[11] S. T. Shishavan and F. S. Gharehchopogh, "An improved cuckoo search optimization algorithm with genetic algorithm for community detection in complex networks," *Multimedia Tools and Applications*, vol. 81, no. 18, pp. 25205–25231, Jul. 2022, https://doi.org/10.1007/s11042-022-12409-x.

[12] F. S. Gharehchopogh, "An Improved Harris Hawks Optimization Algorithm with Multi-strategy for Community Detection in Social Network," *Journal of Bionic Engineering*, vol. 20, no. 3, pp. 1175–1197, May 2023, https://doi.org/10.1007/s42235-022-00303-z.

[13] D. Segera, M. Mbuthia, and A. Nyete, "An Excited Binary Grey Wolf Optimizer for Feature Selection in Highly Dimensional Datasets," in *17th International Conference on Informatics in Control, Automation and Robotics*, Online, 2025, pp. 125–133, https://doi.org/10.5220/0009805101250133.

[14] A. Saxena, B. P. Soni, R. Kumar, and V. Gupta, "Intelligent Grey Wolf Optimizer – Development and application for strategic bidding in uniform price spot energy market," *Applied Soft Computing*, vol. 69, pp. 1–13, Aug. 2018, https://doi.org/10.1016/j.asoc.2018.04.018.

[15] S. K. Goudos, T. V. Yioultsis, A. D. Boursianis, K. E. Psannis, and K. Siakavara, "Application of New Hybrid Jaya Grey Wolf Optimizer to Antenna Design for 5G Communications Systems," *IEEE Access*, vol. 7, pp. 71061–71071, 2019, https://doi.org/10.1109/ACCESS.2019.2919116.

[16] S. Mirjalili, S. M. Mirjalili, and A. Lewis, "Grey Wolf Optimizer," *Advances in Engineering Software*, vol. 69, pp. 46–61, Mar. 2014, https://doi.org/10.1016/j.advengsoft.2013.12.007.

[17] H. R. Tizhoosh, "Opposition-Based Learning: A New Scheme for Machine Intelligence," in *International Conference on Computational Intelligence for Modelling, Control and Automation and International Conference on Intelligent Agents, Web Technologies and Internet Commerce*, Vienna, Austria, 2005, pp. 695–701, https://doi.org/10.1109/CIMCA.2005.1631345.

[18] S. Rahnamayan, H. R. Tizhoosh, and M. M. A. Salama, "Opposition versus randomness in soft computing techniques," *Applied Soft Computing*, vol. 8, no. 2, pp. 906–918, Mar. 2008, https://doi.org/10.1016/j.asoc.2007.07.010.

[19] K. Hussain, M. N. M. Salleh, S. Cheng, and Y. Shi, "On the exploration and exploitation in popular swarm-based metaheuristic algorithms," *Neural Computing and Applications*, vol. 31, no. 11, pp. 7665–7683, Nov. 2019, https://doi.org/10.1007/s00521-018-3592-0.

[20] B. Morales-Castaneda *et al.*, "Handling stagnation through diversity analysis: A new set of operators for evolutionary algorithms," in *2022 IEEE Congress on Evolutionary Computation*, Padua, Italy, 2022, pp. 1–7, https://doi.org/10.1109/CEC55065.2022.9870284.

[21] M. A. Abdelghany, A. A. Ibrahim, H. A. Mohamed, and E. Tammam, "Compact Sub-6 GHz Four-Element Flexible Antenna for 5G Applications," *Electronics*, vol. 13, no. 3, Feb. 2024, Art. no. 537, https://doi.org/10.3390/electronics13030537.

[22] S. Ullah, Y. He, and Y. Huang, "A Triband Circular-Polarized Four-Port MIMO Antenna With Compact Size and Low Mutual Coupling," *IEEE Antennas and Wireless Propagation Letters*, vol. 24, no. 3, pp. 621–625, Mar. 2025, https://doi.org/10.1109/LAWP.2024.3510132.

[23] E. Suganya, T. Prabhu, S. Palanisamy, and A. O. Salau, "Design and performance analysis of L-slotted MIMO antenna with improved isolation using defected ground structure for S-band satellite application," *International Journal of Communication Systems*, vol. 37, no. 16, Nov. 2024, Art. no. e5901, https://doi.org/10.1002/dac.5901.

[24] D. S. Marotkar and P. Zade, "Bandwidth enhancement of microstrip patch antenna using defected ground structure," in *2016 International Conference on Electrical, Electronics, and Optimization Techniques*, Chennai, India, 2016, pp. 1712–1716, https://doi.org/10.1109/ICEEOT.2016.7754978.

[25] S. Sarade and S. D. Ruikar, "Development of a Wide Bandwidth Massive Eight Dissimilar Radiating Element Multiband MIMO Antenna for mm-Wave Application," *Engineering, Technology & Applied Science Research*, vol. 12, no. 5, pp. 9166–9171, Oct. 2022, https://doi.org/10.48084/etasr.5133.

[26] M. M. Nahas and M. Nahas, "Bandwidth and Efficiency Enhancement of Rectangular Patch Antenna for SHF Applications," *Engineering, Technology & Applied Science Research*, vol. 9, no. 6, pp. 4962–4967, Dec. 2019, https://doi.org/10.48084/etasr.3014.

[27] M. J. Hakeem and M. M. Nahas, "Improving the Performance of a Microstrip Antenna by Adding a Slot into Different Patch Designs," *Engineering, Technology & Applied Science Research*, vol. 11, no. 4, pp. 7469–7476, Aug. 2021, https://doi.org/10.48084/etasr.4280.

[28] C. A. Balanis, *Antenna Theory: Analysis and Design*, 3rd ed. Hoboken, NJ, USA: John Wiley & Sons, 2005.